Available online at www.sciencedirect.com
SCIENCE DIRECT
Bioorganic & Medicinal Chemistry
Bioorganic & Medicinal Chemistry 14 (2006) 4217–4226

Structure basis for the inhibitory mechanism of a novel DNase γ-specific inhibitor, DR396

Satoshi Sunaga,[a,b] Atsushi Yoshimori,[c] Daisuke Shiokawa[a] and Sei-ichi Tanuma[a,b,c,*]

[a]*Department of Biochemistry, Faculty of Pharmaceutical Sciences, Tokyo University of Science, 2641 Yamazaki Noda, Chiba 278-8510, Japan*
[b]*Genome and Drug Research Center, Tokyo University of Science, 2641 Yamazaki Noda, Chiba 278-8510, Japan*
[c]*Institute for Theoretical Medicine, Inc. 1-1-5-504 Uchikanda Chiyoda-ku, Tokyo 191-0047, Japan*

Received 10 December 2005; revised 25 January 2006; accepted 26 January 2006
Available online 29 March 2006

Abstract—DNase γ, a member of the DNase I family, has been suggested to cause DNA fragmentation during apoptosis. We recently identified 4-(4,6-dichloro-[1,3,5]-triazine-2-ylamino)-2-(6-hydroxy-3-oxo-3*H*-xanthen-9-yl)-benzoic acid (DR396) as a novel specific inhibitor for human DNase γ [Sunaga, S.; Kobayashi, T.; Yoshimori, A.; Shiokawa, D.; Tanuma, S. *Biochem. Biophys. Res. Commun.* **2004**, *325*, 1292]. However, the binding mode (coordinate) of DR396 to DNase γ has not yet been defined. Here, we examined the molecular basis for the inhibitory activity of DR396 to DNase γ by structure-based computational docking studies. In the blind-docking study using a human DNase γ homology model, a unique binding site of DR396 was predicted, which is tentatively named the 'DNA trapping site' because of the binding domain of the unhydrolyzed DNA strand, but not the active site. Targeting the DNA trapping site as a hot spot, new human DNase γ inhibitors were obtained from our diverse chemical library in silico. These inhibitors showed high correlations between their predicted binding-free energies (ΔGs) and observed IC_{50} values in the DNA trapping site but not the active site. The IC_{50} of a regioisomer of DR396, 5-(4,6-dichloro-[1,3,5]-triazine-2-ylamino)-2-(6-hydroxy-3-oxo-3*H*-xanthen-9-yl)-benzoic acid (DF365), was 73 μM ($\Delta G = -9.75$ kcal/mol), a 20-fold weaker inhibitory ability than that of DR396 (IC_{50} = 3.2 μM, $\Delta G = -11.22$ kcal/mol). Fluorescein and triazine derivatives, partial structures of DR396, had little inhibitory activity for DNase γ. Docking analyses of the interaction between DR396 and DNase γ revealed that DR396 binds tightly to three subsites (S1, S2, and S3) in the trapping site of DNase γ by forming six hydrogen bonds, whereas DF365 and the partial structures are unable to form hydrogen bonds at all three subsites. These findings suggest that the specificity and potency of the inhibitory activity of DR396 for DNase γ is due to the specific interaction of DR396 with three subsites in the DNA trapping site of DNase γ.

1. Introduction

DNase γ, a member of the DNase I family, is a 33 kDa Ca^{2+}/Mg^{2+}-dependent endonuclease.[1,2] It shows high activity under neutral pH conditions and is strongly inhibited by certain metal ions such as Zn^{2+} and Ni^{2+}. The level of DNase γ expression is high in some lymphoid organs, such as liver, spleen, and bone marrow.[2] Its physiological role has been suggested to be the catalysis of nucleosomal DNA fragmentation during apoptosis.[1,2]

Apoptosis is a cellular mechanism for eliminating unwanted cells and harmful cells from the cell community to maintain tissue homeostasis of multicellular organisms.[3,4] One of the outstanding hallmarks of apoptosis is the cleavage of genomic DNA into oligonucleosomal fragments.[5,6] At present, several mammalian DNases, including CAD/DFF40, DNase γ/DNAS1L3, and endonuclease G, have been suggested to be involved in the process of oligonucleosomal DNA fragmentation during apoptosis.[2,7–11] In recent studies, DNase γ has been shown to be indispensable for DNA fragmentation in the differentiation-induced apoptosis of myoblasts and neurons.[12,13] Furthermore, DNA fragmentation in neural apoptosis is catalyzed by either CAD or DNase γ depending on the differentiation status.[13] However, it remains controversial whether the apoptotic DNase differs depending on cell types, cell growth/differentiation status, and/or apoptotic stimulus.

Keywords: DNase γ; Inhibitor; DNA trapping site; Structure–activity relationship.
* Corresponding author. Tel.: +81 4 7124 1501; fax: +81 4 7121 3620; e-mail: tanuma@rs.noda.tus.ac.jp

0968-0896/$ - see front matter © 2006 Elsevier Ltd. All rights reserved.
doi:10.1016/j.bmc.2006.01.073

In a recent study, DNase γ was also suggested to be involved in the generation of resected double-strand DNA breaks (DSBs) associated with somatic hypermutation (SHM).[14] SHM of immunoglobulin (Ig) variable (V) region genes occurs in the germinal center (GC) B cells during immune responses, depending on activation-induced cytidine deaminase (AID). SHM is associated with resected DSBs, which have been shown to occur specifically in rearranged V regions in GC B cells and CD40-simulated B cells expressing AID.[15–20] Importantly, DNase γ is one candidate for the endonucleases responsible for DSBs.[14]

To understand the physiological role of DNase γ by a chemical knockdown strategy, we searched for potent and specific inhibitors of human DNase γ from our chemical library using DNase γ-stable transfectants of HeLa S3 cells (HeLa-γ cells) by evaluating the suppression of apoptotic DNA fragmentation catalyzed by DNase γ, and found a novel DNase γ-specific inhibitor, DR396 (Fig. 1).[21] The IC_{50} value of DR396 for recombinant human DNase γ was calculated to be 3.2 μM. Furthermore, DR396 was shown to be more potent on DNase γ than DNase I ($IC_{50} > 300$ μM). Moreover, DR396 was found to inhibit nucleosomal DNA fragmentation catalyzed by DNase γ during apoptosis. Therefore, DR396 could provide a valuable tool for investigating the biological functions of DNase γ. Furthermore, DR396 may become an attractive lead compound for generating more effective inhibitors optimized for DNase γ.[21] However, the molecular mechanism by which DR396 inhibits DNase γ has not yet been resolved.

In this study, we investigated the structural basis for the specific interaction of DR396 with DNase γ. We predicted a unique binding site of DR396 (tentatively named 'DNA trapping site') by the blind-docking study using the human DNase γ homology model. Furthermore, by targeting the trapping site as a hot spot, new DNase γ inhibitors were obtained. These inhibitors were revealed to have high correlations between their predicted binding-free energies (Δ*G*s) and observed IC_{50} values to the trapping site but not the active site. These observations clearly show that the potent and selective inhibitory activity of DR396 is due to the specific binding of DR396 to the unique DNA trapping site on DNase γ. Furthermore, these results point out the importance of the DNA trapping site as a hot spot for the rational design of optimized DNase γ inhibitors.

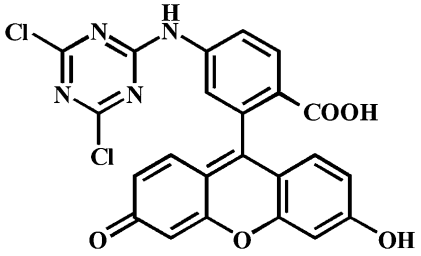

Figure 1. Chemical structure of DR396. DR396; 4-(4,6-dichloro-[1,3,5]-triazine-2-ylamino)-2-(6-hydroxy-3-oxo-3*H*-xanthen-9-yl)-benzoic acid.

2. Results

2.1. Construction of a human DNase γ homology model

To analyze the molecular basis for the inhibition of human DNase γ by DR396, we first built a 3D-structure of human DNase γ by the homology modeling method. Among DNase I family members (DNase I, DNase γ, DNase X, and DNAS1L2), the 3D-structure of only bovine DNase I has been solved.[22–25] Since amino acid homology between human DNase γ and bovine DNase I is 47%, construction of a homology model of human DNase γ using the bovine DNase I structure as a template is practicable. In some solved structures of bovine DNase I, the DNase I–DNA complex structure was selected as a template because of the important information about the interaction sites between DNase I and DNA. Of two structures of the bovine DNase I–DNA complex (Protein Data Bank Accession Codes 1DNK and 2DNJ), we selected the 2DNJ (2 Å) structure, which has a higher resolution than that of 1DNK (2.3 Å).[24,25]

On the basis of 2DNJ DNase I structure and multiple alignments of DNase I family members (Fig. 2A), we constructed a human DNase γ homology model. Superpositions of the bovine DNase I structure and the human DNase γ homology model are shown in Figure 2B. We next performed energy minimization of the model for the complex state of human DNase γ with DNA, and the sequence-structure compatibility of the model was checked using the Verify 3D program. The Verify 3D profiles of the structures of bovine DNase I and human DNase γ are shown in Figure 2C. The predicted structure of human DNase γ was revealed to have an acceptable 3D–1D self-compatibility score (=127), since it is beyond the incorrect fold score threshold (=116). The threshold (*S*) was calculated with the following equation, $S = \exp(-0.83 + 1.008 \ln(L))$, where *L* is a length of residues of the protein.[26]

2.2. Prediction of the DR396 binding site on DNase γ by a blind-docking study

To examine the binding site of DR396 on DNase γ, the homology model of DNase γ was used and a blind-docking study was performed. When there is no prior knowledge of the binding site for small molecules on a target protein, a blind-docking study is a useful method to identify some possible complexes based on an evaluation of binding-free energies (Δ*G*s). The efficiency of a blind-docking study using the Autodock program has been demonstrated in a previous report.[27]

Using the blind-docking study, we attempted to predict a possible binding site for DR396 on DNase γ. As a result of a study involving 100 runs, eight clusters were obtained (Fig. 3A). The cluster is defined as a mass of conformations having RMSD (root mean square deviation) less than 2 Å in the AutoDock3.0 program. The

A

```
                                                1
Human  DNase γ  -20   MSRE---LAPLLLLLLSIHSALAMRICSFNVRSFGESKQEDKNAMDVIVKVIKRCDIILVMEIKDSNNRICPILMEKLNRNSRRGITYNYVISSRLGRKT
Human  DNase I  -22   MRG-MKLLGALLALAALLQGAVSLKIAAFNIQTFGETKMSNATLVSYIVQILSRYDIALVQEVRDSHLTAVGKLLDNLNQDAPD--TYHYVVSEPLGRNS
Human  DNase X  -18   MHYPTALL-----FLILANGAQAFRICAFNAQRLTLAKVAREQVMDTLVRILARCDIMVLQEVVDSSGSAIPLLLRELNRFDGSG-PYSTLSSPQLGRST
Human  DNAS1L2  -18   MGGPRALLAALWALEA--AGTAALRIGAFNIQSFGDSKVSDPACGSIIAKILAGYDLALVQEVRDPDLSAVSALMEQINSVSEH--EYSFVSSQPLGRDQ
Bovine DNase I  -22   MRG-TRLMGLLLALAGLLQLGLSLKIAAFNIRTFGETKMSNATLASYIVRIVRRYDIVLIQEVRDSHLVAVGKLLDYLNQDDPN--TYHYVVSEPLGRNS
                      *      .     .     .. . .* .** . .  .*         . ...   *. ...*. *.       *.  .*        *  . *  ***

                                                                                                          135
Human  DNase γ   78   YKEQYAFLYKEKLVSVKRSYHYHDYQDG-DADVFSREPFVVWFQSPHTAVK--------------------DFVIIPLHTTPETSVKEIDELVEVYTDVK
Human  DNase I   76   YKERYLFVYRPDQVSAVDSYYYDDGCEPCGNDTFNREPAIVRFFSRFTEVR--------------------EFAIVPLHAAPGDAVAEIDALYDVYLDVQ
Human  DNase X   77   YMETYVYFYRSHKTQVLSSYVYND-----EDDVFAREPFVAQFSLPSNVLP--------------------SLVLVPLHTTPKAVEKELNALYDVFLEVS
Human  DNAS1L2   79   YKEMYLFVYRKDAVSVVDTYLYPD-----PEDVFSREPFVVKFSAPGTGERAPPLPSRRALTPPPLPAAAQNLVLIPLHAAPHQAVAEIDALYDVYLDVI
Bovine DNase I   76   YKERYLFLFRPNKVSVLDTYQYDDGCESCGNDSFSREPAVVKFSSHSTKVK--------------------EFAIVALHSAPSDAVAEINSLYDVYLDVQ
                      * * * . ..        .* * *       * * *** .  *                                . ...**..*     *.. * .*. .*
                                                                                                                      254
Human  DNase γ  157   HRWKAENFIFMGDFNAGCSYVPKKAWKNIRLRTDPRFVWLIGDQEDTTVKKSTNCAYDRIVLRGQEIVSSVVPKSNSVFDFQKAYKLTEEEALDVSDHFP
Human  DNase I  156   EKWGLEDVMLMGDFNAGCSYVRPSQWSSIRLWTSPTFQWLIPDSADTTAT-PTHCAYDRIVVAGMLLRGAVVPDSALPFNFQAAYGLSDQLAQAISDHYP
Human  DNase X  152   QHWQSKDVILLGDFNADCASLTKKRLDKLELRTEPGFHWVIADGEDTTVRASTHCTYDRVVLHGERCRSLL--HTAAAFDFPTSFQLTEEEALNISDHYP
Human  DNAS1L2  174   DKWGTDDMLFLGDFNADCSYVRAQDWAAIRLRSSEVFKWLIPDSADTTVG-NSDCAYDRIVACGARLRRSLKPQSATVHDFQEEFGLDQTQALAISDHFP
Bovine DNase I  156   QKWHLNDVMLMGDFNADCSYVTSSQWSSIRLRTSSTFQWLIPDSADTTAT-STNCAYDRIVVAGSLLQSSVVPGSAAPFDFQAAYGLSNEMALAISDHYP
                      . *   . ...*****.*. .       . *..   * *.* *  ***    ..*.***.*  *      .   .    .*   . * .  *  .***.*

Human  DNase γ  257   VEFKLQSSRAFTNSKKSVTLRKKTKSKRS------
Human  DNase I  255   VEVMLK-----------------------------
Human  DNase X  250   VEVELKLSQAHSVQPLSLTVLLLLSLLSPQLCPAA
Human  DNAS1L2  273   VEVTLKFHR--------------------------
Bovine DNase I  255   VEVTLT-----------------------------
                      **  *.
```

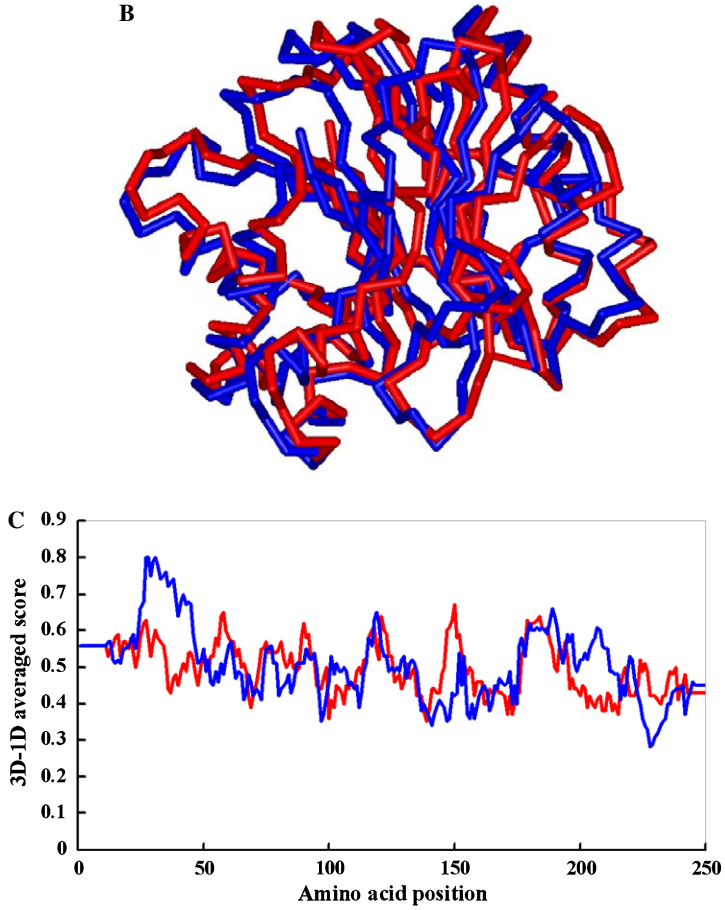

Figure 2. Homology model of human DNase γ. (A) Multiple alignment of DNase I family members used for building the model. Alignment was generated using the Clustal X program as described in Section 4. Identical and conserved residues are indicated by asterisks and dots, respectively. Two conserved His residues (possible active site) are shown by bold letters. The GenBank accession numbers of human DNase γ, DNase I, DNase X, DNAS1L2, and bovine DNase I are U75744, M55983, X90392, U62647, and AJ001538, respectively. (B) Superposition of the crystal structure of bovine DNase I (red) and the homology model of human DNase γ (blue). The model for human DNase γ was constructed using the MODELLER program. The protein Data Bank accession code for the bovine DNase I used as a template for modeling is 2DNJ. Superposition of structures and energy minimization were performed using the Profit program and AMBER94 program, respectively, as described in Section 4. (C) Verify 3D profiles of the bovine DNase I structure (red) and the model for human DNase γ (blue). The predicted structure of human DNase γ has an acceptable 3D–1D self-compatibility score (=127) beyond the incorrect fold score threshold (=116).

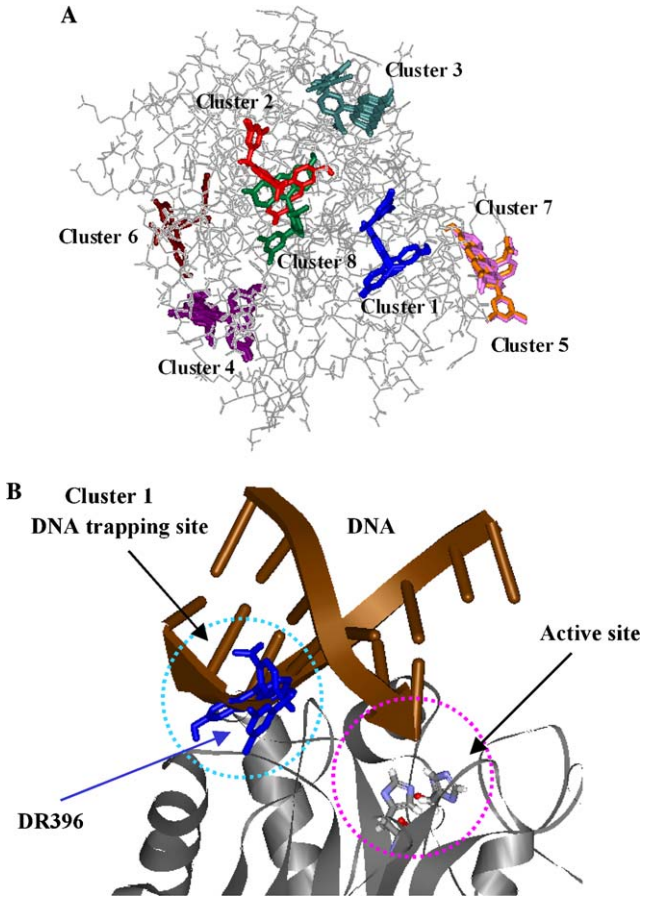

Figure 3. Predicted binding site of DR396 on DNase γ. (A) The binding site of DR396 on DNase γ was predicted by a blind-docking study as described in Section 4. The eight clusters thus obtained were numbered in order of their Δ*G*s. (B) Cluster 1, which has the lowest docked energy, represents a unique DNA binding site, the 'DNA trapping site,' and not the active site. DR396 (blue) and two His in the active site are shown in stick models. The backbone carbons, nitrogens, and oxygens of His are shown in gray, blue, and red, respectively.

cluster ranks based on Δ*G*s and the number of conformations during 100 runs are summarized in Table 1. Since the location of DR396 in cluster 1 has the lowest Δ*G*, we defined it as the most practicable binding site on DNase γ. Interestingly, this site is a unique DNA binding site for the unhydrolyzed DNA strand, but is not the active site. The unique DNA binding site is tentatively named the 'DNA trapping site' (Fig. 3B).

Table 1. Results of blind-docking study of DR396 on DNase γ

Cluster rank	Δ*G* (kcal/mol)	Number of conformations in the cluster
1	−10.51	3
2	−9.87	3
3	−9.84	3
4	−9.65	14
5	−9.58	4
6	−9.36	5
7	−9.28	3
8	−9.26	4

2.3. Specific interaction of DR396 with the DNA trapping site on DNase γ

To further examine that the DNA trapping site on DNase γ is the real binding site for DR396, we compared Δ*G* values between the DNA trapping site and the active site calculated by a docking study in Autodock3.0. Each docking simulation was performed with the DNA trapping site or the active site as the center of coordinates as described in Section 4.

The Δ*G* of DR396 on the DNA trapping site was calculated to be −11.22 kcal/mol. On the other hand, the Δ*G* of DR396 on the active site was calculated to be −9.48 kcal/mol. Apparently, the affinity of DR396 for the DNA trapping site is higher than that for the active site. To understand the differences of Δ*G* values between the DNA trapping site and the active site, we compared in silico the binding modes (coordinates) of DR396 on these two sites. The DNA trapping site on DNase γ is mainly composed of three subsites (S1, S2, and S3) (Fig. 4A). DR396 is predicted to bind strongly to the center of these subsites by forming six hydrogen bonds with residues in the subsites (Ser10, Glu13, Asn44, Arg72, Thr77, and Gln81). The fluorescein of DR396 binds to the S1 and S2 subsites, and the triazine group binds to the S3 subsite.

On the other hand, DR396 is predicted to form only two hydrogen bonds with the active site of DNase γ. Furthermore, the predicted binding mode of DR396 on the active site is not the center of the pocket (Fig. 4B). Thus, these results suggest that the true binding site of DR396 is the DNA trapping site, but not the active site.

2.4. Screening of new DNase γ-specific inhibitors using the DNA trapping site as a hot spot

The above results and the fact of the low homology between human DNase γ and bovine DNase I in the trapping site (52%) compared to the active site (85%) allow us to find new DNase γ-specific inhibitors by targeting the DNA trapping site. So, we screened candidates from our chemical library of about 100,000 diverse compounds and performed docking simulations with the DNA trapping site of DNase γ. Compounds whose Δ*G* values were lower than −8.5 kcal/mol were selected from the library.

To determine whether these compounds inhibit human DNase γ activity, the inhibitory effects on human recombinant DNase γ activity were evaluated by adding various concentrations to the standard assay mixture containing salmon testis dsDNA as a substrate. The enzyme reaction was performed at 37 °C for 10 min to maintain the linearity of the reaction with less than 30% of the substrate dsDNA being hydrolyzed. In this screening, test compounds whose IC_{50} values were less than 100 μM were defined as active. As shown in Figure 5, 10 compounds were identified as active compounds. Interestingly, DR396 was screened again from our chemical library. Among the active compounds, 5-(4,6-dichloro-[1,3,5]-triazine-2-ylamino)-2-(6-hydroxy-3-oxo-3*H*-xanthen-9-yl)-benzoic acid (DF365) (IC_{50} = 73

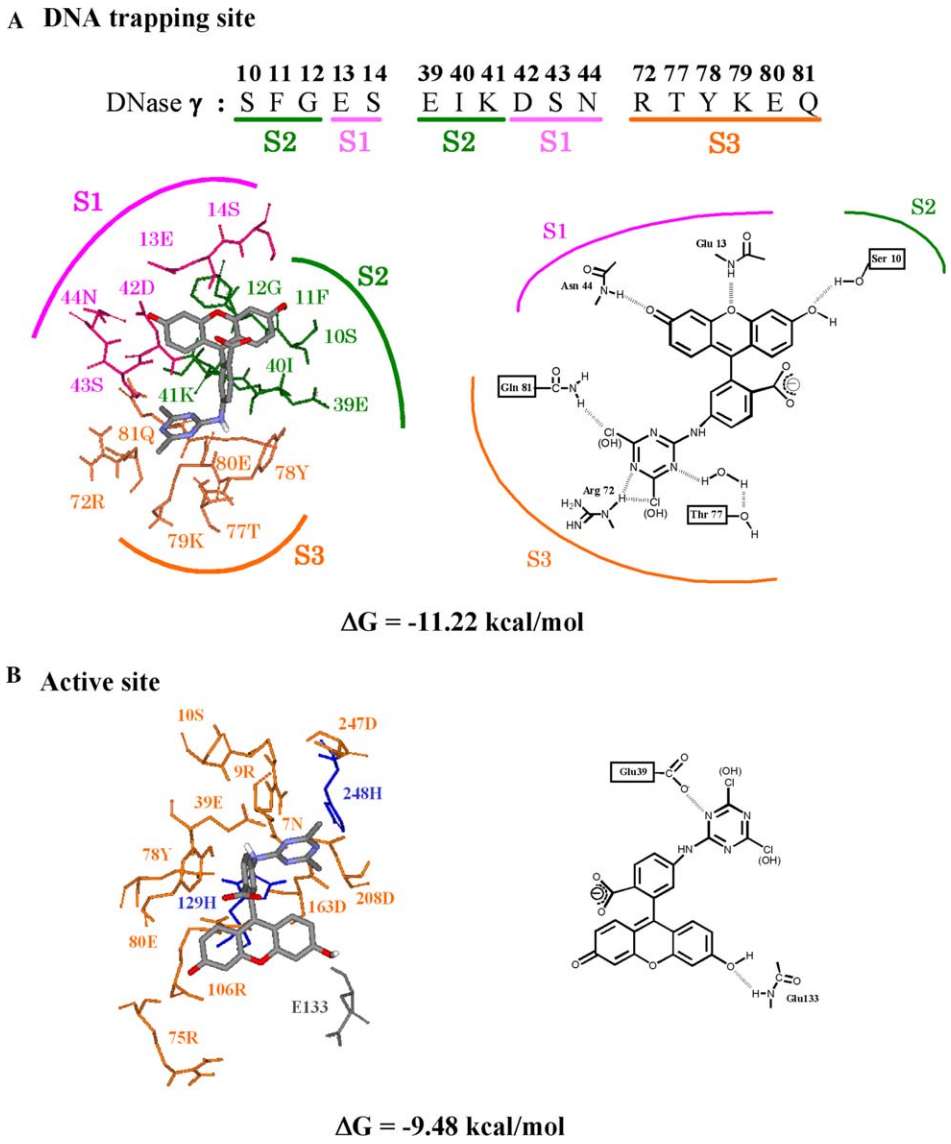

Figure 4. Predicted binding form of DR396 on DNase γ. (A) The Δ*G* value and the binding form to the DNA trapping site on DNase γ were obtained by performing a docking study as described in Section 4. DR396 was predicted to bind at three subsites (S1, S2, and S3) of the DNA trapping site through the formation of six hydrogen bonds. Although the two chlorines in DR396 are probably hydrolyzed, the substitutions do not affect the Δ*G* value or the binding form. The backbone carbons, hydrogens, nitrogens, and oxygens of DR396 are shown in gray, white, blue, and red, respectively. (B) The Δ*G* value and the binding form to the active site on DNase γ were obtained by performing a docking study as described in Section 4. Two active His (blue) and residues belonging to the active site (orange) are shown.

μM) and Eosin Yellowish (IC_{50} = 36 μM) are analogs of DR396. However, their inhibitory activities were weaker than that of DR396 (IC_{50} = 3.2 μM). It is noteworthy that there is a good correlation between their predicted Δ*G*s and their observed IC_{50} values (Fig. 6A). On the other hand, there are no correlations between their predicted Δ*G*s and their observed IC_{50} values in the active site (Table 2 and Fig. 6B). These results indicate that the DNA trapping site is the actual binding site of not only DR396, but also of these inhibitory compounds.

2.5. Structure–activity relationship of DR396 in DNase γ inhibition

It is interesting that DF365, a regioisomer of DR396, was screened as an inhibitory compound (Fig. 5). Although the difference between DF365 and DR396 lies only in the location of triazine group, the DNase γ inhibitory activity differs by over 20-fold (IC_{50} values of DR396 and DF365 are 3.2 and 73 μM, respectively). The predicted Δ*G* values of DR396 and DF365 are −11.22 and −9.75 kcal/mol, respectively, and the difference in the Δ*G* values between DR396 and DF365 is 1.47 kcal/mol (Fig. 7A).

To understand the molecular basis for the difference, we conducted a computational analysis of the binding modes of DR396 and DF365 on the DNA trapping site of DNase γ. As shown in Figure 7B, DF365 is unable to form hydrogen bonds with the S3 subsite of the DNA trapping site of DNase γ. Thus, the lower inhibitory activity of DF365 is probably due to the difference in

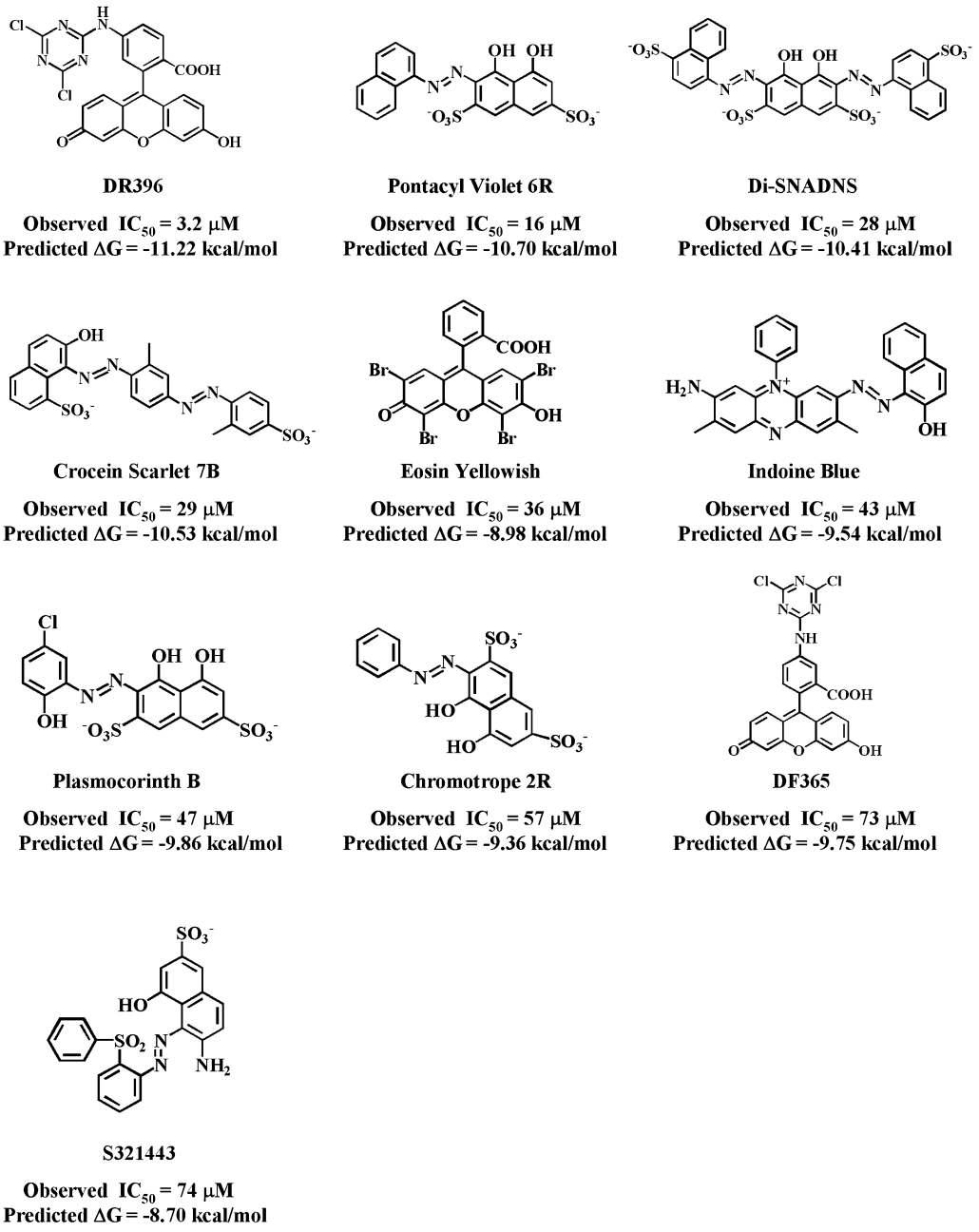

Figure 5. New DNase γ inhibitors obtained by screening using the DNA trapping site as a hot spot. Compounds with Δ*G*s lower than −8.5 kcal/mol were screened from our chemical library, which contains about 100,000 diverse compounds. The compounds that fulfilled the threshold were evaluated by an in vitro DNase γ inhibition assay. The docking simulation and in vitro inhibition assay were performed as described in Section 4. Values are averages of three independent experiments.

the location of the triazine group, which results in a lower affinity (Figs. 4A and 7B).

Next, we examined the inhibitory effects of other partial structures (fluorescein, (4,6-dichloro-[1,3,5]-triazine-2-yl)-phenyl amine (R282049), 2-amino-4,6-dichloro-*s*-triazine, and *s*-triazine) of DR396 (Fig. 8A). All compounds showed little inhibitory activity against DNase γ even at a concentration of 100 μM. The docking simulation of these compounds on the DNA trapping site of DNase γ showed the Δ*G* values of these compounds to be very high as compared with those of DR396 and DF365 (Figs. 7A and 8A). The binding modes of fluorescein and triazine are shown in Figure 8B. These compounds are unable to bind to the DNA trapping site with the same configuration as DR396. Taken together, the good correlations between the predicted Δ*G* values and their binding modes and the observed inhibitory activities of DR396 analogs suggest that the DNA trapping site of DNase γ is the true binding site for DR396.

3. Discussion

We previously found a novel inhibitor of DNase γ, DR396, but it remains unclear how DR396 causes the

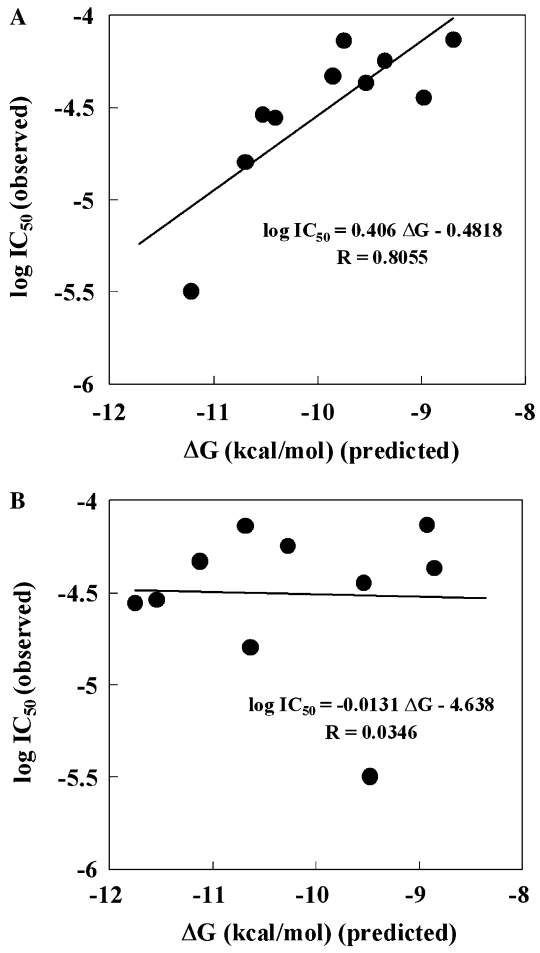

Figure 6. Correlations between the predicted Δ*G*s and IC_{50} values of DNase γ inhibitors on (A) DNA trapping site and (B) active site. The predicted Δ*G*s were calculated by the docking simulation as described in Section 4. The IC_{50} values were determined by an in vitro inhibition assay as described in Section 4. The solid line shows a linear regression fit, and *R* denotes the correlation coefficient. The RMSD values between actual log IC_{50} values and predicted log IC_{50} values from a linear regression fit are (A) 0.226 and (B) 0.382, respectively.

Table 2. Predicted Δ*G*s of compounds on active site of DNase γ

Compounds	Δ*G* (kcal/mol)	IC_{50} (μM)
DR396	−9.48	3.2
Pontacyl Violet 6R	−10.64	16
Di-SNADNS	−11.76	28
Crocein Scarlet 7B	−11.55	29
Eosin Yellowish	−9.54	36
Indoine Blue	−8.86	43
Plasmocorinth B	−11.13	47
Chromotrope 2R	−10.28	57
DF365	−10.69	73
S321443	−8.93	74
Fluorescein	−9.26	>100
R282049	−6.73	>100
2-Amino-4,6-dichloro-*s*-triazine	−4.30	>100
s-Triazine	−3.53	>100

specific inhibition of DNase γ. In this study, to obtain information on the structural basis for the specific interaction between DR396 and DNase γ, computational docking studies were performed. Since the DNase γ crystal structure has not yet been solved, we constructed a human DNase γ homology model with an acceptable 3D–1D self-compatibility score beyond the incorrect fold score threshold (Fig. 2). This homology model has no negative score regions on the Verify3D profile, and the profile wave is not inferior to that of bovine DNase I, which was used as a template crystal structure. This is not unexpected since there is a high degree of amino acid conservation between bovine DNase I and human DNase γ (47%), and a high resolution template structure was used. The high quality homology model could be the basis for the success of the computational analyses.

Using the homology model, we first investigated the binding site of DR396 on DNase γ. As a method for finding binding pockets on a protein molecule without any prior knowledge, we utilized a blind-docking study using the Autodock program. This program has been shown to be able to predict correct complexes based on energy for not only rigid ligands, but also flexible ligands.[27] In the blind-docking study of DR396 on DNase γ, no clusters with high affinity for the center of the active site were obtained (Fig. 3A). Also the affinity (Δ*G* evaluation) of DR396 for the active site was revealed to be very low (Fig. 4B). Importantly, the other DNA binding site (DNA trapping site) was predicted to be the highest affinity binding site (Figs. 3 and 4A). The binding affinity of DR396 for the DNA trapping site was calculated to be high due to the formation of six hydrogen bonds with three subsites (S1, S2, and S3) (Fig. 4A). These results indicate that DR396 binds to the unique DNA trapping site on DNase γ but not to the active site.

To obtain support for the above idea, we searched for other new DNase γ inhibitors by screening our chemical library using the DNA trapping site as a hot spot. From our chemical library of about 100,000 diverse compounds, we found 10 inhibitors with predicted high affinities for the DNA trapping site of DNase γ. These inhibitors, which include DR396 and its analogs, show high correlation between their predicted binding energies (Δ*G*s) and observed IC_{50} values to the DNA trapping site but not the active site (Fig. 6). These observations suggest that DR396 binds specifically to the DNA trapping site.

To confirm the specific binding of DR396 to the DNA trapping site of DNase γ, the structure–activity relationship of DR396 analogs was analyzed computationally (Figs. 7 and 8). The inhibitory activity of DF365, which is a regioisomer of DR396, was about 20-fold lower (IC_{50} = 73 μM) than that of DR396 (IC_{50} = 3.2 μM). The weak inhibitory activity of DF365 was revealed to be due to a weak binding capacity for the S3 pocket of the DNA trapping site (Fig. 7B). Expectedly, fluorescein and triazine derivatives, partial structures of DR396 that are predicted to have lower affinities for the DNA trapping site, had no inhibitory effect on DNase γ, even at 100 μM (Fig. 8). These results strongly suggest that DR396 binds solely to the DNA trapping site of DNase γ.

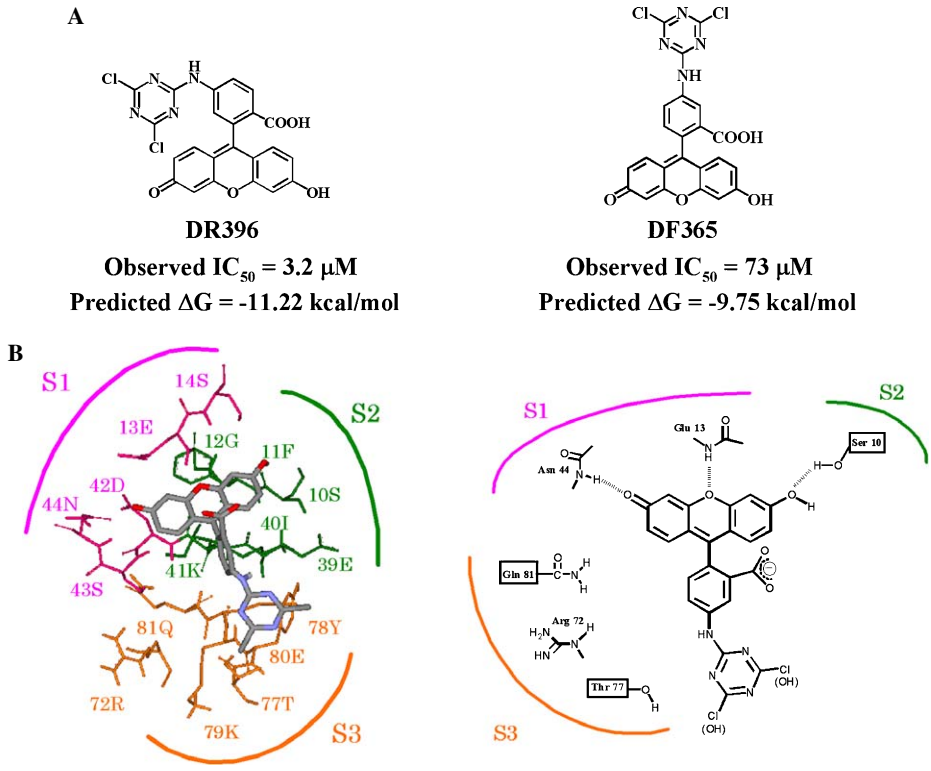

Figure 7. Effect of DF365, a regioisomer of DR396, on DNase γ. (A) IC_{50} values and the predicted Δ*G*s of DR396 and DF365. DF365; 5-(4,6-dichloro-[1,3,5]-triazine-2-ylamino)-2-(6-hydroxy-3-oxo-3*H*-xanthen-9-yl)-benzoic acid. The docking simulation and in vitro inhibition assay were performed as described in Section 4. Values are the averages of three independent experiments. (B) Predicted binding form of DF365 on the DNA trapping site of DNase γ. DF365 is unable to bind to the S3 subsite of the DNA trapping site. The backbone carbons, hydrogens, nitrogens, and oxygens of each compound are shown in gray, white, blue, and red, respectively.

In summary, we conclude that the molecular basis of the specific inhibitory activity of DR396 against DNase γ is due to specific binding to the DNA trapping site on DNase γ. This implies that new DNase γ-specific inhibitors could be screened and designed by targeting the DNA trapping site as a hot spot. Studies are in progress to screen for more effective DNase γ-specific inhibitors using our computational screening system. Structural knowledge about the amino acid residues required for the specific interaction between DR396 and DNase γ might be expected to simplify the design of small molecular inhibitors.

4. Experimental

4.1. Materials

4-(4,6-Dichloro-[1,3,5]-triazine-2-ylamino)-2-(6-hydroxy-3-oxo-3*H*-xanthen-9-yl)-benzoic acid (DR396), sodium 6-amino-5-(2-benzenesulfonyl-phenylazo)-4-hydroxy-naphthalene-2-sulfonate (S321443), and (4,6-dichloro-[1,3,5]-triazine-2-yl)-phenyl amine (R282049) were purchased from Sigma–Aldrich Library of Rare Chemicals. Pontacyl Violet 6R was from Tokyo Kasei Kogyo Co., Ltd. Di-SNADNS and Eosin Yellowish were from Lancaster synthesis. Indoine Blue, Plasmocorinth B, and fluorescein were from Aldrich. Crocein Scarlet 7B, Chromotrope 2R, and *s*-triazine were from Sigma. 5-(4,6-Dichloro-[1,3,5]-triazine-2-ylamino)-2-(6-hydroxy-3-oxo-3*H*-xanthen-9-yl)-benzoic acid (DF365) was from Fluka. 2-Amino-4,6-dichloro-*s*-triazine was from Toronto Research Chemicals, Inc.

4.2. Preparation of human recombinant DNase γ

The human recombinant DNase γ was made by the pET15b vector (Novagen). The cDNA fragment encoding the mature DNase γ protein was obtained by PCR using 5′-ATATAT**TCATGA**GAATCTGCTCCTTCA ACG-3′(sense) and 5′-TATAT**GGATCC**CTAAGTGA CAGATTTTTTG-3′ (anti-sense) primers, with the *Bsp*HI (sense) and *Bam*HI (anti-sense) sites flanking the coding sequences shown in bold letters. After the fragments were excised by *Bsp*HI and *Bam*HI digestion, they were subcloned into the *Nco*I/*Bam*HI sites of pET15b vector. The recombinant human DNase γ protein was expressed in Rosetta (DE3) cells, and refolded and purified from inclusion bodies. Briefly, inclusion bodies containing recombinant DNase γ were dissolved in buffer (40 mM Tris–HCl, 10 mM DTT, pH 7.5) containing 8 M urea and then refolded by dilution to 0.08 M urea. The recombinant DNase γ was purified by affinity column chromatography on Heparin-5PW (Tosho) as described previously.[28]

4.3. Assay of DNase γ activity

DNase γ activity was assayed by measuring the increase in acid-soluble DNA that remains unprecipitated in the

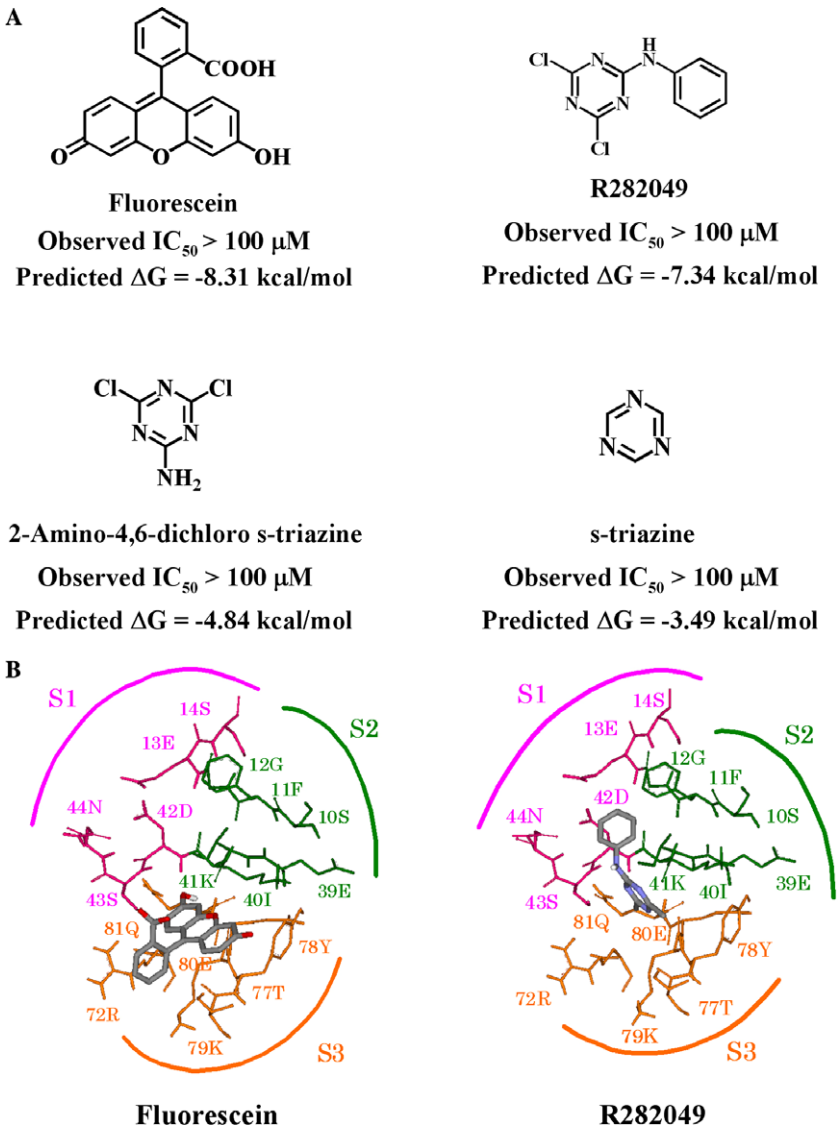

Figure 8. Effect of DR396 analogs on DNase γ. (A) IC_{50} values and predicted Δ*G*s of DR396 analogs. The docking simulation and in vitro inhibition assay were performed as described in Section 4. Values are the averages of three independent experiments. (B) Predicted binding forms of fluorescein and (4,6-dichloro-[1,3,5]-triazine-2-yl)-phenyl amine (R282049) on the DNA trapping site of DNase γ. These structures are too small to bind to the trapping site in the same form as DR396. The backbone carbons, hydrogens, nitrogens, and oxygens of each compound are shown in gray, white, blue, and red, respectively.

presence of 5% perchloric acid (PCA) as described previously.[29] Briefly, 0.8 Kunitz U/ml of DNase γ was incubated with inhibitor in the standard assay buffer (50 mM Mops–NaOH, 3 mM $CaCl_2$, 3 mM $MgCl_2$, and 0.1 mg/ml BSA, pH 7.2) at 37 °C for 30 min. Then, 0.5 mg/ml of double-stranded salmon testis DNA (dsDNA) was added, and the mixture was incubated at 37 °C. The reaction was terminated by the addition of 5% PCA and leaving the mixture on ice for 20 min. After centrifugation at 800*g* for 15 min at 4 °C, the absorbance of the supernatant at 260 nm was measured.

4.4. Building a DNase γ homology model

The amino acid sequences of human DNase I family members and bovine DNase I were retrieved from the GenBank database (accession numbers of human DNase γ, human DNase I, human DNase X, human DNAS1L2, and bovine DNase I are U75744, M55983, X90392, U62647, and AJ001538, respectively). The sequences were aligned using the ClustalX program[30] and then adjusted manually. A multiple alignment using the BLOSUM matrix series,[31] a gap opening penalty of 11.0, and a gap extension penalty of 0.05 were chosen to align the sequences. This sequence alignment was used as the basis for homology modeling using the MODELLER program.[32] An X-ray structure of the bovine DNase I–DNA complex (Brookhaven Protein Data Bank Accession Code 2DNJ) was used as a template for modeling. The complex structure of human DNase γ/DNA was constructed by superposition over the structure of DNase I–DNA using the McLachlan algorithm as implemented in the ProFit program.[33,34] Then, the protein was subjected to energy minimization using the AMBER94 program with the steepest descent algorithm.[35] The sequence-structure compatibility of the

protein model was checked using the Verify 3D program.[26] Molecular visualization was carried out in DS ViewerPro (Accelrys, Inc., San Diego, CA).

4.5. Ligands

All ligands were prepared in CDX format using ChemDraw (CambridgeSoft) and then converted to three-dimensional structures and energy minimized in Chem3D (Cambridge Soft). The carboxyl and amino acid groups of the ligands were ionized, since this is the form in which they usually occur under physiological conditions. Partial atomic charges for ligands were computed using the Gasteiger–Marsili algorithm.[36]

4.6. Automated docking

The search for putative binding sites for DR396 on DNase γ was performed by a blind-docking approach[27] with the Autodock3.0 Lamarckian Genetic Algorithm[37] on a COMPAQ Alphastation DS20E (double 833 MHz and 1024 MB of memory). The binding-free energy scoring function in the AutoDock is based on an empirical function derived by linear regression analysis of a large set of diverse protein–ligand complexes with known inhibition constants. There are many successful examples of protein–ligand system structures studied by the AutoDock.[38,39] During a docking simulation in AutoDock, the receptor is rigid and fixed while the ligand is flexible and can both translate and rotate. Docking was performed in a 121 Å × 121 Å × 121 Å volume, with grid spacing of 0.550 Å, centered on DNase γ. The number of energy evaluations was set at 1×10^7. Each simulation was performed a total of 100 runs. Other parameters were default values. After docking had been carried out, each docking pose was used to identify putative binding sites. The model with the lowest binding-free energy was selected as a predicted binding site for DR396.

For calculating Δ*G*s on the targeting sites (DNA trapping site and active site), and for predicting the binding mode of each compound, automated docking was performed in a 45 Å × 45 Å × 45 Å volume, with grid spacing of 0.375 Å, centered on the targeting sites of DR396. The number of energy evaluations was set at 5×10^6. Each simulation was performed a total of 10 runs. Other parameters were default values. After docking had been carried out, the lowest-energy docking pose was used for analysis.

Acknowledgment

This work was supported in part by a Grant-in-Aid for Scientific Research from the Ministry of Education, Culture, Sports, Science and Technology of Japan.

References and notes

1. Shiokawa, D.; Ohyama, H.; Yamada, T.; Tanuma, S. *Biochem. J.* **1997**, *326*, 675.
2. Shiokawa, D.; Tanuma, S. *Biochemistry* **2001**, *40*, 143.
3. Kerr, J. F.; Wyllie, A. H.; Currie, A. R. *Br. J. Cancer* **1972**, *26*, 239.
4. Tanuma, S. In *Apoptosis in Normal Development and Cancer*; Sluyser, M., Ed.; Taylor and Francis: London, 1996; pp 39–59.
5. Wyllie, A. H. *Nature* **1980**, *284*, 555.
6. Arends, M. J.; Morris, R. G.; Wyllie, A. H. *Am. J. Pathol.* **1990**, *136*, 593.
7. Liu, X.; Zou, H.; Slaughter, C.; Wang, X. *Cell* **1997**, *89*, 175.
8. Enari, M.; Sakahira, H.; Yokoyama, H.; Okawa, K.; Iwamatsu, A.; Nagata, S. *Nature* **1998**, *391*, 43.
9. Nagata, S.; Nagase, H.; Kawane, K.; Mukae, N.; Fukuyama, H. *Cell Death Differ.* **2003**, *10*, 108.
10. Parrish, J.; Li, L.; Klotz, K.; Ledwich, D.; Wang, X.; Xue, D. *Nature* **2001**, *412*, 90.
11. Li, L. Y.; Luo, X.; Wang, X. *Nature* **2001**, *412*, 95.
12. Shiokawa, D.; Kobayashi, T.; Tanuma, S. *J. Biol. Chem.* **2002**, *277*, 31031.
13. Shiokawa, D.; Tanuma, S. *Cell Death Differ.* **2004**, *11*, 1112.
14. Okamoto, M.; Okamoto, N.; Yashiro, H.; Shiokawa, D.; Sunaga, S.; Yoshimori, A.; Tanuma, S.; Kitamura, D. *Biochem. Biophys. Res. Commun.* **2005**, *327*, 76.
15. Rajewsky, K. *Nature* **1996**, *381*, 751.
16. Storb, U.; Shen, H. M.; Michael, N.; Kim, N. *Philos. Trans. R. Soc. Lond. B Biol. Sci.* **2001**, *356*, 13.
17. Neuberger, M. S.; Milstein, C. *Curr. Opin. Immunol.* **1995**, *7*, 248.
18. Woo, C. J.; Martin, A.; Scharff, M. D. *Immunity* **2003**, *19*, 479.
19. Muramatsu, M.; Sankaranand, V. S.; Anant, S.; Sugai, M.; Kinoshita, K.; Davidson, N. O.; Honjo, T. *J. Biol. Chem.* **1999**, *274*, 18470.
20. Muramatsu, M.; Kinoshita, K.; Fagarasan, S.; Yamada, S.; Shinkai, Y.; Honjo, T. *Cell* **2000**, *102*, 553.
21. Sunaga, S.; Kobayashi, T.; Yoshimori, A.; Shiokawa, D.; Tanuma, S. *Biochem. Biophys. Res. Commun.* **2004**, *325*, 1292.
22. Oefner, C.; Suck, D. *J. Mol. Biol.* **1986**, *192*, 605.
23. Kabsch, W.; Mannherz, H. G.; Suck, D.; Pai, E. F.; Holmes, K. C. *Nature* **1990**, *347*, 37.
24. Lahm, A.; Suck, D. *J. Mol. Biol.* **1991**, *222*, 645.
25. Weston, S. A.; Lahm, A.; Suck, D. *J. Mol. Biol.* **1992**, *226*, 1237.
26. Bowie, J. U.; Luthy, R.; Eisenberg, D. *Science* **1991**, *253*, 164.
27. Hetenyi, C.; van der Spoel, D. *Protein Sci.* **2002**, *11*, 1729.
28. Shiokawa, D.; Iwamatsu, A.; Tanuma, S. *Arch. Biochem. Biophys.* **1997**, *346*, 15.
29. Kunitz, M. *J. Gen. Physiol.* **1940**, *24*, 15.
30. Thompson, J. D.; Higgins, D. G.; Gibson, T. J. *Nucleic Acids Res.* **1994**, *22*, 4673.
31. Henikoff, S.; Henikoff, J. G. *Proc. Natl. Acad. Sci. U.S.A.* **1992**, *89*, 10915.
32. Sali, A.; Blundell, T. L. *J. Mol. Biol.* **1993**, *234*, 779.
33. Martin, A. C. R. <http://www.bioinf.org.uk/software/profit/>.
34. McLachlan, A. D. *Acta Crystallogr. A* **1982**, *38*, 871.
35. Cornell, W. D.; Cieplak, P.; Bayly, C. I.; Gould, I. R.; Merz, K. M.; Ferguson, D. M.; Spellmeyer, D. C.; Fox, T.; Caldwell, J. W.; Kollman, P. A. *J. Am. Chem. Soc.* **1995**, *117*, 5179.
36. Gasteiger, J.; Marsili, M. *Tetrahedron* **1980**, *36*, 3219.
37. Morris, G. M.; Goodsell, D. S.; Halliday, R. S.; Huey, R.; Hart, W. E.; Belew, R. K.; Olson, A. J. *J. Comput. Chem.* **1998**, *19*, 1639.
38. Bartolucci, C.; Perola, E.; Pilger, C.; Fels, G.; Lamba, D. *Proteins: Struct. Funct. Genet.* **2001**, *42*, 182.
39. Jenkins, J. L.; Shapiro, R. *Biochemistry* **2003**, *42*, 6674.